Dynamic Finger Gaits via Pivoting and Adapting Contact Forces

Yuechuan Xue   Ling Tang   Yan-Bin Jia

Department of Computer Science

Iowa State University

Ames, IA 50011, USA

`yuechuan,ling,jia@iastate.edu`

Abstract— **For over three decades finger gaiting has remained largely a subject for theoretical inquiries. Successful execution of a sequence of finger gaits does not simply reduce to planning collision-free paths for the involved fingers. A major issue is how to move the gaiting finger without losing other finger contacts with the object. To realize the finger movement, it will most likely undergo a motion as the contact forces must be adapted during the gait. This paper focuses on a single finger gait executed on a tool by an anthropomorphic hand driven by an arm. To improve stability, the tool's tip is leveraged as a pivot on the supporting plane. The gait consists of three stages: removal, during which the contact force on the gaiting finger gradually decreases to zero; relocation, during which the finger follows a pre-planned path (relative to the moving object) to establish a new contact; and addition, during which the contact force on the relocated finger increases to some desired level. Hybrid position/impedance control employ reference finger forces that satisfy the friction cone constraints and are dynamically consistent with the object's motion, which in turn provides reference poses for the fingertips to maintain their contacts during the gait. Finger gaits have been demonstrated on a kitchen knife and a screwdriver with an Adept SCARA robot and a Shadow Dexterous Hand.**
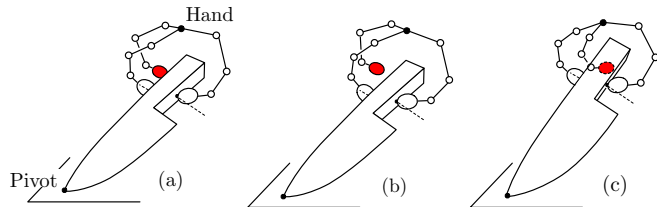
Fig. 1: Single finger gait. (a) The fingertip marked in red is about to be removed from the handle as its contact force gradually decreases to 0. (b) The fingertip is being relocated to a new contact position. (c) The fingertip re-establishes contact with the handle from the bottom side, increasing its contact force gradually to a certain level.

I. INTRODUCTION

Until today, no algorithms exist for a robotic hand to achieve power grasps on naturally resting tools. Several issues surrounding a successful grasp execution have often been overlooked in research. First, part of a tool's handle may not be accessible because the tool often lies on a supporting surface instead of standing on it or being hanged in the air. Consequently, some pre-grasp operations are needed. Second, finger gaits need to be carried out to achieve a desired relative pose of the hand to the handle. This requires planning of the motions of the tool and hand along with the finger contact forces under dynamics and contact constraints. The resulting position and force trajectories can then be used as profiles for control and execution. Third, primitive operations, such as gaits and pivots, are vital for preventing loss of finger contact.

We are interested in hand tools with pointed tips (e.g., kitchen knives, screwdrivers, wrenches). A kitchen knife will be focused on as a representative in this paper, but the analysis and control methods can be easily transferred to other tools. A sequence of finger gaits is performed dynamically by an anthropomorphic hand mounted on an arm. Each gait breaks down into three stages: *finger removal*, *finger relocation*, and *finger addition*, as shown in Fig. 1. Contrary to a common presumption, finger removal cannot

be performed in negligible time because this may cause other fingers to slip at their contacts. We aim for a procedure that gradually reduces the contact force to zero on the finger being detached. In some poses, the knife will inevitably move with the change of this contact force, since the static equilibrium and friction cone constraints cannot be satisfied simultaneously. Consequently, a knife pivoting motion is carried out to dynamically balance the object and adapt the contact forces on the other gripping fingers to prevent slippage.

During relocation, the finger establishes a new contact via tracking some pre-planned path. Unlike previous studies [1]–[4], the palm is allowed to move for achieving a larger range of motion and, as a result, yielding fewer gaits towards the goal grasp. Addition of the finger, as opposed to removal, increases the contact force on it to a certain level. Optimization is employed to cope with the force indeterminacy caused by the presence of multiple contact points.

The paper is organized as follows. Section III derives the dynamics of the knife in a pivoting motion. To reduce the disturbance to the object due to finger removal and addition, a strategy for smooth contact force adjustments is proposed in Section IV. In Section V, a path of the entire hand during finger relocation is generated using the rapidly-exploring random tree (RRT) algorithm [5]. Section VI develops a workspace hybrid position/impedance controller for the arm-hand system, with the objectives to apply a desired force, and in the meantime, to prevent the fingers from sliding or rolling on the handle. Section VII presents finger gaiting experiments on a kitchen knife and a screwdriver with an Adept SCARA robot and Shadow Dexterous Hand. Section VIII concludes with some discussion and future work.

II. RELATED WORK

A. Finger Gaiting

Though proposed more than three decades ago [3], finger gaiting has remained mostly a subject for theoretical inquiry with simulation based on often unrealistically simplified hand models [1], [4]. The maneuver is especially useful when a dexterous manipulation cannot be accomplished by rolling or sliding without violating constraints such as workspace limits, force balance requirements, etc. Much of the existing research has focused on planning one or more finger gaits given the object's trajectory. In [3], [4], a finger gait was performed when the fingers were reaching their workspace limitations, while the remaining fingers maintained a force closure grasp. Manipulation involving finger gaits is sometimes modeled as a hybrid (discrete/continuous) system [1], where path planning algorithms are applied to find a better finger trajectories, at a high computational cost. Many researchers have also made attempts in the hand hardware design [6], [7]. Either the mechanical structure is sometimes oversimplified to hardly operate on objects beyond simple toys, or there is a strong dependence on accurate knowledge of the geometry of the fingers and object. There are relatively few studies concerning robust finger gait control in the presence of uncertainties and perturbations during an execution [2], [8]–[11].

B. Pivoting

Pivoting involves rotating a constrained object relative to a contact point with the environment or one of the fingers. Extrinsic resources [12], such as gravity and the supporting force from the environment, have been utilized by the maneuver as complements to hand dexterity. This line of research started with controlled object slipping in the hand [13], and followed with quasi-static pivoting of polyhedral objects on the supporting plane [14], [15]. More recent works use dynamics to generate large rotations [16], and utilize friction [17] and soft finger contact [18] to implement robust control strategies against uncertainties. Reinforcement learning was also exploited in [19] to generate a model free pivoting control strategy.

C. Object Motion Control

Hand manipulation such as grasping or finger gaiting relies on accurate finger positioning and force control. To deal with contact constraints, controls of force and position are more effectively carried out in the workspace. In particular, hybrid force/position control [20] is effective when the object being manipulated is fixed in the direction of the controlled force, since the implicit force-displacement relationship can be satisfied. When the object is movable, impedance control, which adjusts the force indirectly through specifying the impedance of the grasped object against the external force [21]–[23], can achieve a better balance between the accuracies of position and force controls. The desired force distribution is often obtained by optimization [24] due to the presence of multiple contacts, using a cost function such as power consumption by joint actuators [26] or joint torques for external wrench resistance [25].

III. DYNAMICS OF KNIFE PIVOTING

A kitchen knife lies on the table to be picked up by a robotic hand (mounted on an arm). To attain a power grasp of the knife's handle, the hand first needs to gain full access to its surface. The strategy is to first lift the handle up via pivoting the knife. Finger gaits can then performed to achieve such a grasp. This section focuses on the initial pivoting. The following assumptions are made throughout the paper:

1) The knife has known mass properties and shape.
2) The knife's initial pose is available to the algorithm.
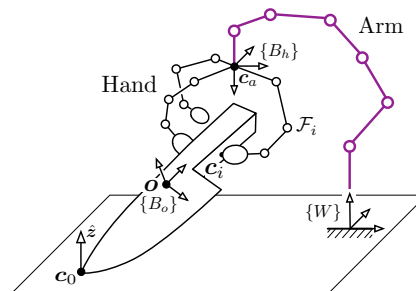3) Point contact model with Coulomb's friction.

Fig. 2: Arm-hand mechanism.

As shown in Fig. 2, the tip c_0 of the knife's blade is chosen as the pivot. Two fingers are in contact with antipodal points $^b c_1$ and $^b c_2$ on the knife's handle, respectively. Here, the superscript b refers to the knife's body frame $\{B_o\}$ located at its center of mass o.

We pre-specify a target orientation of the knife after the lift-up and plan its orientation trajectory $R_o(t)$ using the SLERP [35] algorithm with some trapezoidal velocity profile. Here, R_0 is the matrix describing the orientation of $\{B_0\}$ relative to the world frame $\{W\}$ located at the arm's base (see Fig. 2). Since the pivot point c_0 stays motionless, the knife's position in the world frame $\{W\}$ is given as

$$o = c_0 - R_o\,{}^b c_0. \qquad (1)$$

Differentiating (1) with respect to time twice, we have

$$\dot{v} = -[\dot{\omega}]_\times R_o\,{}^b c_0 - [\omega]_\times[\omega]_\times R_o\,{}^b c_0. \qquad (2)$$

where $v, \omega \in \mathbb{R}^3$ are the knife's linear and angular velocities in $\{W\}$, and the operator $[\cdot]_\times$ yields an anti-symmetric matrix whose product with any 3-vector equals the cross product of the operand with that vector.

We proceed by calculating the desired contact forces that are required for the knife to move along a lifting trajectory without breaking its contact with any finger or the table. These forces will serve as reference values for a controller to be described later on.

Denote by $f_0 \in \mathbb{R}^3$ the contact force exerted by the table and $f_i \in \mathbb{R}^3$, $i = 1, 2$ be that by the finger $\mathcal{F}_i$, all subject

to Coulomb friction. Utilizing (2), the dynamics of the knife can be represented in terms of $\dot{\boldsymbol{\omega}}$ as

$$M_o\dot{\boldsymbol{\omega}} + C_o = G\boldsymbol{f}, \tag{3}$$

where G is the grasp matrix and $\boldsymbol{f} = (\boldsymbol{f}_1^\top, \boldsymbol{f}_2^\top)^\top$.

In rigid body dynamics, a redundancy of contacts results in indeterminacy of contact forces. To address this issue, a subsequent constrained optimization problem is solved at each time step of lifting:

$$\max_{\boldsymbol{f}_0,\boldsymbol{f}_1,\boldsymbol{f}_2} \sum_{i=0}^{2} \left(\hat{\boldsymbol{n}}_i^\top \hat{\boldsymbol{f}}_i\right)^2. \tag{4}$$

The objective function characterizes the overall deviation of the contact forces from their respective contact normals.

The optimization (4) is subject to several constraints. The first one is the dynamics equation (3), where $\boldsymbol{\omega}$ and $\dot{\boldsymbol{\omega}}$ are obtained by differentiating the prescribed trajectory $R_o(t)$. Next, every contact force $\boldsymbol{f}_i$ must stay inside its friction cone, namely,

$$\|\boldsymbol{f}_i - (\boldsymbol{f}_i^\top \hat{\boldsymbol{n}}_i)\hat{\boldsymbol{n}}_i\| \le \mu_i \boldsymbol{f}_i^\top \hat{\boldsymbol{n}}_i, \qquad i = 0, 1, 2, \tag{5}$$

where $\mu_0 = \mu_T$ and $\mu_i = \mu_H, i = 1, 2$, are the coefficients of friction at the table and finger contacts. Finally, the normal component of each contact force lies within a range:

$$f_{n,\min} \le \boldsymbol{f}_i^\top \hat{\boldsymbol{n}}_i \le f_{n,\max}, \qquad i = 0, 1, 2 \tag{6}$$

where the bounds $f_{n,\min}$ and $f_{n,\max}$ ensure that the force is large enough to maintain contact despite uncertainties but not too large to break the finger. An interior point optimization solver [34] can be employed to solve (4).

IV. SMOOTH CONTACT FORCE ADJUSTMENT

In this section, we consider how to smoothly remove or establish a finger contact on the knife's handle, so as to avoid the instability otherwise caused by sudden changes in contact forces. For convenience, we denote $\mathcal{F}_3$ as the finger to be removed or added, and $\mathcal{F}_1, \mathcal{F}_2$ as the fingers whose contacts on the knife's handle need to be maintained.

A. Finger Removal

Removal of $\mathcal{F}_3$ reduces the number of contact points by one. The knife often needs to be "dynamically balanced" via a motion to keep the forces at the remaining contacts to be inside their friction cones. We intend to allow minimum knife reorientation to be performed simultaneously with contact force adjustments.

Let the finger $\mathcal{F}_3$ adjust from its initial value of $\boldsymbol{f}_{3,0}$ to $\boldsymbol{0}$ to completely separately the contact. Due to continuous adjustment of the force $\boldsymbol{f}_3$ exerted by $\mathcal{F}_3$, the contact force on the table or one of $\mathcal{F}_1$ and $\mathcal{F}_2$ may reach the edge of its friction cone to yield a slip (and eventually a break of contact). To prevent this from happening and thus keep the knife constrained, we propose a dynamic equilibrium-based force adjustment strategy. It allows the knife to rotate about the pivot $\boldsymbol{c}_0$ in a controlled manner.

We simultaneously optimize both knife's pivoting trajectory and the corresponding contact forces. The trajectory is

(a) Finger removal.
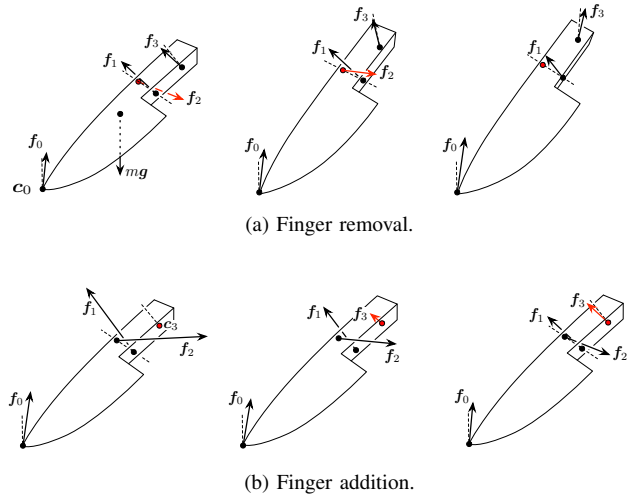

(b) Finger addition.

Fig. 3: From left to right, the plots show the contact forces at the beginning, in the middle, and at the end of their adjustments for (a) removing the finger $\mathcal{F}_3$ or (b) adding the finger $\mathcal{F}_2$. Gradual adjustments of forces on the three fingers result in knife movements.

uniformly discretized into K steps over a fixed duration. Each iteration k is associated with a fixed set of variables, including a unit quaternion $\boldsymbol{r}_k$ that represents the knife's orientation, an angular velocity $\boldsymbol{\omega}_k$, an angular acceleration $\boldsymbol{\sigma}_k$, and four contact forces $\boldsymbol{f}_{i,k}$, $i = 0, \ldots, 3$, all at time instant k. The cost function C to be minimized has the form:

$$C = \delta(\boldsymbol{r}_0, \boldsymbol{r}_K) + \lambda_1 \sum_{k=0}^{K} \boldsymbol{\sigma}_k^\top \boldsymbol{\sigma}_k - \lambda_2 \sum_{k=1}^{K} \sum_{i=0}^{3} (\hat{\boldsymbol{f}}_{i,k}^\top \hat{\boldsymbol{n}}_{i,k})^2,$$

where $\delta(\boldsymbol{r}_0, \boldsymbol{r}_K)$ is the angle between the knife's initial and final orientation, and λ_1, λ_2 the weights of the corresponding costs.

Among the constraints enforced at each iteration are the knife's dynamics equation (3) and the friction cone constraints (5) and (6). Additionally, the Euler integral constraints are assigned to each step:

$$\boldsymbol{r}_{k+1} = \frac{1}{2}h\boldsymbol{\omega}_k\boldsymbol{r}_k, \quad \boldsymbol{\omega}_{k+1} = \boldsymbol{\omega}_k + h\boldsymbol{\sigma}_k,$$

where h is the time step size. We also impose boundary conditions $\boldsymbol{\omega}_0 = \boldsymbol{\omega}_K = \boldsymbol{0}$, $\boldsymbol{\sigma}_K = \boldsymbol{0}$, which require the knife to stop at a steady state. Next, all quaternion variables must have unit norms. The last constraint ensures a linear decay of the contact force on the removing finger:

$$\boldsymbol{f}_{3,k}^\top \hat{\boldsymbol{n}}_{3,k} = \left(1 - \frac{k}{K}\right) \boldsymbol{f}_{3,0}^\top \hat{\boldsymbol{n}}_{3,0}. \tag{7}$$

Due to the complexity of this optimization, proper initialization of the free variables is necessary to find a solution. We gradually scale up the problem by doubling the step number K each round and apply linear interpolation of the results from the previous round to initialize variables in the next. Fig. 4 shows some planned contact force trajectories simulated using MuJoCo [33].
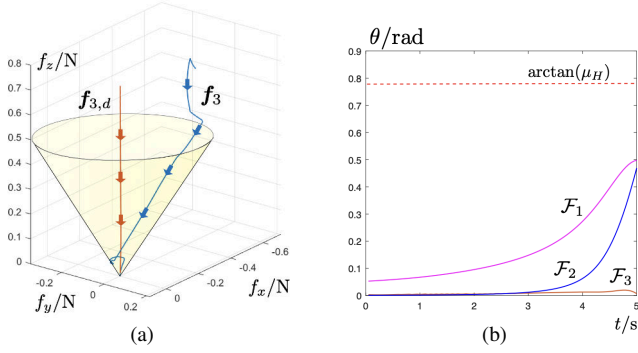
Fig. 4: Simulation result of finger removal. (a) Contact force trajectory of the removing finger within the friction cone. (b) The angles between contact forces and the normal.

B. Finger Addition

This phase starts after the finger $\mathcal{F}_3$ reaches the new location on the handle. With the new contact, the knife's gravitational load needs to be redistributed. We first calculate a desired load distribution by solving an optimization problem similar to (4) with an additional contact force $\boldsymbol{f}_3$ being considered. The knife is kept static during the entire period. Thus, its angular velocity and acceleration are both set to zero. We denote the optimal forces by $\boldsymbol{f}_{i,d}$, $i = 1, 2, 3$.

We consider adjusting the contact force by the finger $\mathcal{F}_3$ from $\boldsymbol{0}$ to its target value of $\boldsymbol{f}_{3,d}$ to achieve a smooth establishment of contact. Suppose addition of $\mathcal{F}_3$ takes L time periods (mapped to control cycles) of equal duration h. We let the normal component of $\boldsymbol{f}_3$ increase linearly to $f_{3,nd} = \boldsymbol{f}_{3,d}^\top \hat{\boldsymbol{n}}_3$ where $\hat{\boldsymbol{n}}_3$ is the inward normal of the object at the contact. More specifically, at step l, $0 \le l \le L$, we solve the optimization problem (4) with $i = 0, \ldots, 3$ and an additional linear constraint

$$\boldsymbol{f}_3^\top \hat{\boldsymbol{n}}_3 = \frac{l}{L} f_{3,nd}. \tag{8}$$

V. FINGER REPOSITIONING

The gaiting finger $\mathcal{F}_3$ needs to reposition itself to reach a new contact location on the knife's handle. This happens either right after its removal from an old contact location, or when the finger makes the first ever contact with the handle. In this section, we look at how to plan a relocation trajectory for the finger.

The hand is moved by a 6-DOF arm. We let $\boldsymbol{\xi}_h \in \mathbb{R}^6$ be the palm's pose, and for $i = 1, 2, 3$, $\boldsymbol{q}_i$ be the joint angles of the finger $\mathcal{F}_i$. The palm's pose is determined by the vector $\boldsymbol{q}_h$ which consists of the joint angles allocated from the hand to the palm and the joint angles of the arm. Denote by $\boldsymbol{q}_{h,\text{start}}$ the starting configuration of the palm for finger repositioning. The goal configuration $\boldsymbol{q}_{h,\text{goal}}$ is obtained through inverse kinematics from a target contact point ${}^b\boldsymbol{c}_3$ on the knife's handle. This point is supplied by a higher-level planner of gaits[1]. The configuration $\boldsymbol{q}_{h,\text{goal}}$ should not create a collision between the knife and hand.

[1]Design of this planner is part of our future work.

A. Constraints on Fingertips

As shown in the Fig. 5, the tip of every finger $\mathcal{F}_i$, $1 \le i \le 3$, has a body frame $\{B_i\}$ located at its geometric center $\boldsymbol{o}_i$. Let $\{B_{i,d}\}$ denote the fingertip's desired frame. For every finger $\mathcal{F}_i$ we introduce two frames $\{C_i\}$ and $\{T_i\}$ fixed on the fingertip and knife's handle, respectively. In the case that $\mathcal{F}_i$ is in contact with the handle, the two frames are both located at the contact point $\boldsymbol{c}_i$ where their z-axes are respectively aligned with the handle's outward and inward normals. In the case that $\mathcal{F}_i$ is being repositioned, $\{C_i\}$ and $\{T_i\}$ will achieve the aforementioned alignment once the finger comes into contact with the handle.
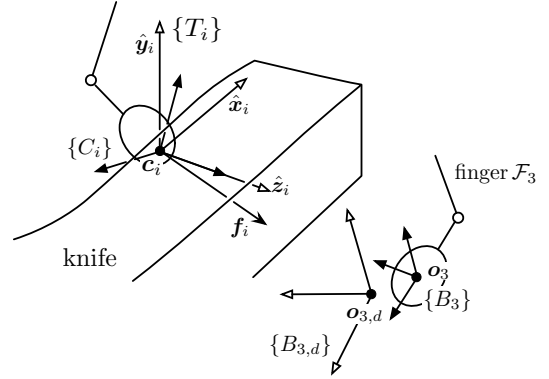

Fig. 5: Frames $\{T_i\}$ and $\{C_i\}$ for finger $\mathcal{F}_i$.

Here, we define the finger $\mathcal{F}_i$'s local coordinates $\boldsymbol{\xi}_i$ as a 6-dimensional vector comprising three Z-Y-X Euler angles $(\theta_i, \psi_i, \phi_i)^\top$ and three translational coordinates $(x_i, y_i, z_i)^\top$. When the finger is in contact with the knife, $\boldsymbol{\xi}_i$ describes the relative pose of the contact frame $\{C_i\}$ to the tool frame $\{T_i\}$. If the finger is being repositioned or not being used, $\boldsymbol{\xi}_i$ describes the relative pose of the frame $\{B_i\}$ to $\{B_{i,d}\}$.

For a grasping finger $\mathcal{F}_i$, $i = 1, 2$, to prevent its tip from sliding, the three translational coordinates x_i, y_i, and z_i need to maintain the value 0. Rolling of the fingertip, modeled as a round shape, can be prevented by keeping the Euler angles ψ_i and ϕ_i (about the y_i- and z_i- axes, respectively) at 0. The first Euler angle θ_i, describing a rotation about the contact normal, does not have to be constrained because its change will not affect the contact position on the knife. Under these circumstances, any rotation from $\{C_i\}$ to $\{T_i\}$ is about the $\hat{\boldsymbol{z}}_i$ axis only:

$$R_i^o = R_{x_i}(\phi_i) R_{y_i}(\psi_i) R_{z_i}(\theta_i) = R_z(\theta_i).$$

The above constraint can be represented as follows:

$$S_i J_{i,h} \dot{\boldsymbol{\xi}}_h + S_i J_{i,i} \dot{\boldsymbol{q}}_i = 0, \qquad i = 1, 2 \tag{9}$$

where

$$S_i = [\boldsymbol{0}_{5 \times 1}, I_{5 \times 5}]$$

is a matrix that selects all rotational and translational coordinates but θ_i, $\dot{\boldsymbol{\xi}}_h$ is the velocity of the palm frame, and the analytical Jacobians $(J_{i,h}, J_{i,i})$ together transform the velocity $(\dot{\boldsymbol{\xi}}_h^\top, \dot{\boldsymbol{q}}_i^\top)^\top$ to $\mathcal{F}_i$'s contact frame $\{C_i\}$. From now

on, we refer to $\{C_i\}$ as the *contact frame* and $\{T_i\}$ as the *tool frame* for the finger $\mathcal{F}_i$

B. A Revised RRT Planner

Multiple algorithms exist for the kinodynamic motion planning problem of constructing a path from $\boldsymbol{q}_{h,\text{start}}$ to $\boldsymbol{q}_{h,\text{goal}}$ under the constraint (9), which needs to be satisfied throughout the entire relocation motion to prevent a contact break or movement. Below we briefly describe a modified version of the RRT algorithm.

In one RRT iteration, we randomly sample[2] a pose $T_{3,\text{rand}} \in SE(3)$ of the body frame $\{B_3\}$ and query its nearest neighbor $T_{3,\text{nn}}$ in the RRT search tree. Next, a uniform speed trajectory $T_3(t)$ from $T_{3,\text{rand}}$ to $T_{3,\text{nn}}$ is interpolated via the SLERP algorithm. Differentiating $T_3(t)$, we have the velocity $\dot{\boldsymbol{\xi}}_3$ of the frame $\{B_3\}$, which in the meantime satisfies

$$\dot{\boldsymbol{\xi}}_3 = J_{3,a}\dot{\boldsymbol{\xi}}_h + J_{3,3}\dot{\boldsymbol{q}}_3. \tag{10}$$

The constraints (9) and (10) are stacked together as $A\dot{\boldsymbol{q}}_h = \boldsymbol{b}$, and solved for $\dot{\boldsymbol{q}}_h$ using the null space of A:

$$\dot{\boldsymbol{q}}_h = A^\dagger \boldsymbol{b} + (I - A^\dagger A)\dot{\boldsymbol{q}}_{h,\text{null}},$$

where $A^\dagger$ is the pseudo-inverse of A and

$$\dot{\boldsymbol{q}}_{h,\text{null}} = \delta \nabla \|\boldsymbol{q}_h - \boldsymbol{q}_{h,\text{goal}}\|^2,$$

where δ is a fixed small step size. We propagate the RRT search tree from the nearest state towards the sampled pose $T_{3,\text{rand}}$ on the manifold defined by the constraints (9) and (10). The tree propagation stops when a collision is detected, and then the next RRT iteration starts. If a valid trajectory is returned from the state, add the state to the tree. Continue the search until a goal state is found or some failure criterion is satisfied.

The motion of the desired body frames $\{B_{h,d}\}$ for the palm and $\{B_{3,d}\}$ for the finger $\mathcal{F}_3$ can be determined once a repositioning path is planned. The grasping fingers' task frames $\{T_i\}$, $i = 1, 2$ are fixed on the knife during the motion and their desired contact forces are kept unchanged. A hybrid controller to be introduced in Section VI will carry out the repositioning.

VI. GAITING VIA HYBRID POSITION/IMPEDANCE CONTROL

So far, the knife's motion trajectories and their accompanying contact force trajectories have been constructed for the initial lifting and a complete finger gait. In this section, we present a controller to track these motions and regulate contact forces.

Suppose that the finger $\mathcal{F}_i$ has n_i degrees of freedom (DOFs), for $1 \leq i \leq 3$. The system of the arm and hand has a total of $n = 6 + n_1 + n_2 + n_3$ DOFs, which constitute the system configuration $\boldsymbol{q}$.

[2]with a certain probability (as we try to direct the trajectory toward the final goal)

A. Acceleration for the Relocating Finger

The gaiting finger $\mathcal{F}_3$ needs to follow the pose trajectory planned in Section V. Note that $\boldsymbol{\xi}_i$ consists of three Euler angles and three translational coordinates as given in Section V.

We first rename $\boldsymbol{x}_3$ as $\boldsymbol{s}_3$ to highlight on that all its coordinates are selected for control. Next, we have

$$\dot{\boldsymbol{s}}_3 = \begin{bmatrix} E_3 & \\ & I \end{bmatrix} \begin{bmatrix} R_3^\top & \\ & R_3^\top \end{bmatrix} J_3 \dot{\boldsymbol{q}}. \tag{11}$$

where $J_3 \in \mathbb{R}^{6 \times n}$ is the geometric Jacobian evaluated at $\boldsymbol{o}_3$, R_3 is the matrix of rotation from the body frame $\{B_3\}$ of the finger $\mathcal{F}_3$ to the world frame $\{W\}$, and E_3 maps the angular velocity of $\{B_3\}$ in $\{B_{3,d}\}$ to the corresponding Euler angle rates. For simplicity, we denote $\dot{\boldsymbol{s}}_3 = H_3 \dot{\boldsymbol{q}}_3$. Now, we employ the proportional-derivative (PD) control scheme with the acceleration servo below:

$$\ddot{\boldsymbol{s}}_{3,\text{res}} = \ddot{\boldsymbol{s}}_{3,d} + K_v \dot{\boldsymbol{s}}_{3,e} + K_p \boldsymbol{u}_{3,e}, \tag{12}$$

where K_p, K_v are positive definite gain matrices and $\boldsymbol{s}_{3,e} = \boldsymbol{s}_{3,d} - \boldsymbol{s}_3$. The desired task frame position, velocity, and acceleration $\boldsymbol{s}_{3,d}, \dot{\boldsymbol{s}}_{3,d}, \ddot{\boldsymbol{s}}_{3,d}$ can all be derived from the knife's trajectory $R_o(t)$.

B. Acceleration for the Grasping Fingers

For a grasping finger $\mathcal{F}_i$, $i = 1$ or 2 , we let the coordinates $\boldsymbol{\xi}_i$ describe the relative pose of the contact frame $\{C_i\}$ to the task frame $\{T_i\}$. Position control is applied over a subset of coordinates $\boldsymbol{u}_i = (\psi_i, \phi_i, x_i, y_i)^\top$. In the meantime, impedance control is conducted along the z_i-direction to regulate the contact force. We apply a matrix $S_i = (S_{i,u}^\top, S_{i,z}^\top)^\top \in \mathbb{R}^{5 \times 6}$ to select coordinates $\boldsymbol{s}_i = (\boldsymbol{u}_i^\top, z_i^\top)^\top$, where $\boldsymbol{u}_i = S_{i,u}\boldsymbol{\xi}_i$ and $z_i = S_{i,z}\boldsymbol{\xi}_i$.

The equation relating $\dot{\boldsymbol{s}}_i$ and $\dot{\boldsymbol{q}}$ is given as:

$$\dot{\boldsymbol{s}}_i = S_i \begin{bmatrix} E_i & \\ & I_{3 \times 3} \end{bmatrix} \begin{bmatrix} R_i^\top & \\ & R_i^\top \end{bmatrix} J_i \dot{\boldsymbol{q}}, \tag{13}$$

where J_i is the geometric Jacobian evaluated at $\boldsymbol{c}_i$, R_i is the matrix of rotation from the frame $\{C_i\}$ to the frame $\{T_i\}$, and E_i maps the angular velocity of $\{C_i\}$ in $\{T_i\}$ to the corresponding Euler angle rates. Compared with (11), equation (13) has its right hand side begin with the selection matrix S_i in order to drop the rotation about the contact normal. Similarly, we denote $\dot{\boldsymbol{s}}_i = H_i \dot{\boldsymbol{q}}$.

Position control of the coordinates $\boldsymbol{u}_i$ is done in a similar scheme as (12) with obtained acceleration servo $\ddot{\boldsymbol{u}}_{i,\text{res}}$. We deal with force control along the contact normal. Assume that the material at the contact has linear elastic deformation property. The normal component $f_{i,nd}$ of a contact force is then proportional to the amount of finger penetration z_i along the contact normal $\hat{\boldsymbol{z}}_i$. Therefore, to achieve a certain contact force $f_{i,nd}$, the desired z coordinate value $z_{i,d}$ is $f_{i,nd}/k_e$, where k_e is the stiffness at the contact in the steady state. The servo for the acceleration in the z-direction is given as

$$\ddot{z}_{i,\text{res}} = \ddot{z}_{i,d} + k_m^{-1}(f_{i,nd} - f_{i,n} + k_v \dot{z}_{i,e} + k_p z_{i,e}), \tag{14}$$

where $f_{i,n}$ is the normal component of the contact force reading from the tactile sensor on the fingertip. Stacking $\ddot{\boldsymbol{u}}_{i,\mathrm{res}}$ and $\ddot{z}_{i,\mathrm{res}}$ together as $\ddot{\boldsymbol{s}}_{i,\mathrm{res}}$.

A total of n_s coordinates are selected for the three fingers. As for the palm frame $\{B_h\}$, the last $n - n_s$ coordinates $\boldsymbol{s}_h$ are chosen for motion PD control, yielding $\dot{\boldsymbol{s}}_h = H_h \dot{\boldsymbol{q}}$.

C. Robot Controller

All the selected coordinates are gather into a vector $\boldsymbol{s} = (\boldsymbol{s}_h^\top, \boldsymbol{s}_1^\top, \boldsymbol{s}_2^\top, \boldsymbol{s}_3^\top)^\top$. It has the derivative

$$\dot{\boldsymbol{s}} = H\dot{\boldsymbol{q}}, \tag{15}$$

where $H = (H_h^\top, H_1^\top, H_2^\top, H_3^\top)^\top$ is a square matrix since the number of coordinates selected for control is the same as the DOFs of the system. The matrix is invertible as long as the Jacobians $J_i(\boldsymbol{q})$, $1 \le i \le 3$, are non-singular and the Euler angles are away from their singularities. This allows us to solve for the joint acceleration via differentiating (15), obtaining

$$\ddot{\boldsymbol{q}} = H^{-1}\left(\ddot{\boldsymbol{s}} - \dot{H}\dot{\boldsymbol{q}}\right). \tag{16}$$

The dynamics of the arm-hand system is given as

$$\boldsymbol{\tau} = M(\boldsymbol{q})\ddot{\boldsymbol{q}} + N(\boldsymbol{q}, \dot{\boldsymbol{q}}) + J^\top \boldsymbol{f}, \tag{17}$$

where $\boldsymbol{\tau} \in \mathbb{R}^n$ denotes all the joint torques, $M(\boldsymbol{q})$ is the robot's joint space inertia matrix, $N(\boldsymbol{q}, \dot{\boldsymbol{q}})$ represents the Coriolis, centrifugal, and gravitational torques, and J is the matrix that stacks the robot Jacobians evaluated at $\boldsymbol{c}_i$ and $\boldsymbol{f} = (\boldsymbol{f}_1^\top, \boldsymbol{f}_2^\top, \boldsymbol{f}_3^\top)^\top$. Substituting (16) into (17), we rewrite the robot dynamics in the task space:

$$\boldsymbol{\tau} = MH^{-1}\left(\ddot{\boldsymbol{s}} - \dot{H}\dot{\boldsymbol{q}}\right) + N(\boldsymbol{q}, \dot{\boldsymbol{q}}) + J^\top \boldsymbol{f},$$

and describe the controller as

$$\boldsymbol{\tau}_{\mathrm{ctrl}} = MH^{-1}\left(\ddot{\boldsymbol{s}}_{\mathrm{res}} - \dot{H}\dot{\boldsymbol{q}}\right) + N + J^\top \boldsymbol{f}.$$

Letting $\boldsymbol{\tau}_{\mathrm{ctrl}} = \boldsymbol{\tau}$ in the above two equations, we obtain the error dynamics of $\boldsymbol{u}_i$ and z_i:

$$\ddot{\boldsymbol{u}}_{i,e} + K_v \dot{\boldsymbol{u}}_{i,e} + K_p \boldsymbol{u}_{i,e} = 0, \tag{18}$$

$$k_m \ddot{z}_{i,e} + k_v \dot{z}_{i,e} + k_p z_{i,e} = f_{i,n} - f_{i,nd}. \tag{19}$$

The equations (18) and (19) are asymptotically stable. Even though the contact stiffness k_e may not be known exactly in practice, with an approximation of its value, the proper gains k_m and k_v can be chosen to assume a good transient response of (19).

VII. EXPERIMENT

We implemented the introduced knife pivoting and finger gaiting strategy with an Adept Cobra robot and a Shadow Dexterous Hand. The palm has 6 DOFs, of which 4 are from the arm and 2 are from the hand's wrist joints. For validation purpose, only the thumb, index finger, and middle finger are considered.

Contact force sensing was critical in the experiment. With tactile sensors unavailable, we utilized strain gauge sensors to deduce the contact force at each fingertip. On the
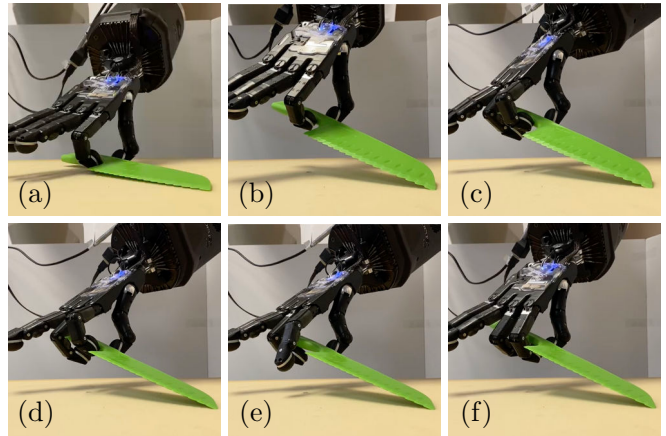

Fig. 6: Finger gaits on a kitchen knife. (a) Initial state with the thumb and index finger placed on the handle. (b) Initial pivoting. (c) Repositioning of the middle finger to the bottom side of the handle and increasing its contact force. (d) Pivoting as the index finger is removed. (e) Success removal of the index finger at the knife's new orientation. (f) Addition of the index finger to a different location.

Shadow Hand, each joint corresponds to a pair of tendons pulling the joint in two opposite directions, and only one tendon is active at a time. We first determined the active tendon via calculating the torque direction at the joint and then converted its strain gauge reading from pulse width modulation (PWM) units to an equivalent joint torque in Nm using a calibration function. This function was obtained by comparing measurements (as ground truth) from a 6-axis force/torque sensor with hand strain gauge readings. The contact position could be inferred from the pose of the knife and the configuration of the robot. With the hand configuration, finger joint torques, and contact point location, the contact force could be derived using the hand's static equilibrium equation. The estimated force deviated less than 25% from the ground truth in terms of magnitude and less than 30 degrees in terms of direction when the hand was in slow motion.

Constrained by the robot programming interface, only position commands could be streamed to the Adept and Shadow hand robot. We used an alternative admittance controller, in which the resolved z coordinate of the grasping finger was computed via

$$z_{i,\mathrm{res}} = z_{i,d} + k_m^{-1}(f_{i,nd} - f_{i,n} + k_p z_{i,e})$$

to mimic the behavior of the hybrid position/impedance control in (14). The task space position commands were transformed to the joint space by an iterative inverse Jacobian solver.

We performed ten trials of the task with the initial pivoting followed by one or two finger gaits for a kitchen knife and a screwdriver, respectively, at different initial resting positions. Fig. 6 and 7 each show two consecutive finger gaits. For the kitchen knife, the robot successfully completed every initial pivoting and first finger gait, though 20% of the experiments
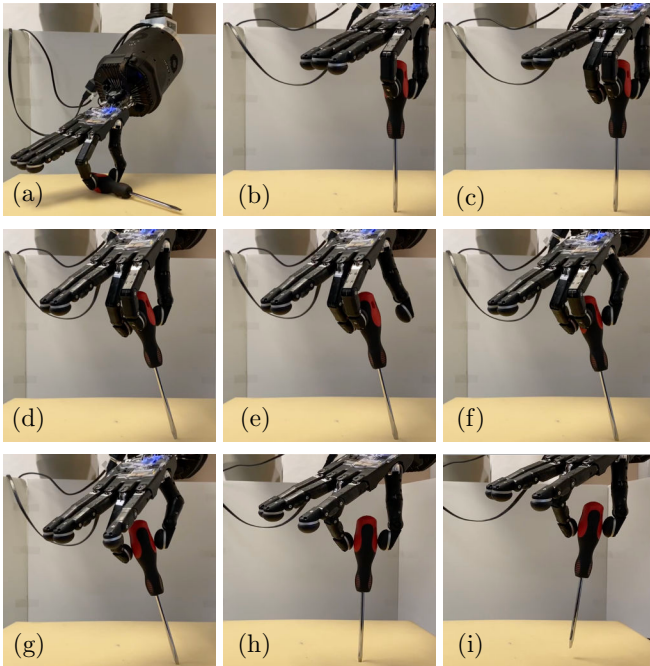
Fig. 7: Finger gaits on a screwdriver. (a)-(b) Initial pivoting of the knife with the thumb and index finger. (c) Addition of the middle finger to the handle surface. (d)-(f) Full finger gait of the thumb, consisting its removal, relocation, and addition. (g)-(i) Removal of the index finger followed by lifting of the screw driver by the thumb and middle finger.
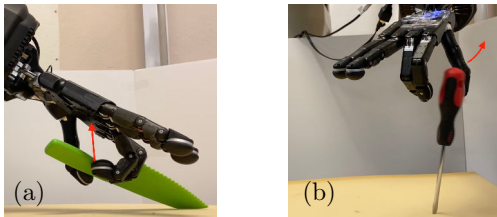

Fig. 8: (a) Under position commands from the hand, the forces acting on the handle cannot be precisely controlled. The middle finger being added slipped on the handle due to excessive contact force and pushes the knife away from the planned pose. (b) Without pivoting, the two grasping fingers fail to balance the weight of the screwdriver as the thumb is removed. The screwdriver inevitably slips out of the control as result.

failed on the second finger gait due to vibration of the arm (Shadow Hand's weight exceeds the payload of the arm) and the lack of visual feedback. Experiments on screwdriver also achieved a 100% success rate on the initial pivoting and first finger gait, and a 50% overall success rate on the second finger gait.

We also found that finger gaits were much more likely to fail if under position commands with no hybrid control or pivoting involved. Two failure cases are shown in Fig. 8.

VIII. Discussion and Future Work

This paper investigates the maneuvering of a hand tool by an anthropomorphic hand with a novel approach that combines pivoting with dynamic balancing to achieve stability

and mechanical simplicity. This is realized by planning not only the tool trajectory but also the trajectories of finger forces to stay consistent with dynamics and contact friction constraints. These profile trajectories are then used by control policies at the bottom level for implementation. At the top level, a finger gait is concluded, with the contact force on the gaiting finger gradually reduced to zero or increased to a desired level. The redistributed contact forces on the other fingers is simultaneously "absorbed" by the tool through pivoting.

As the work deals with the execution of mostly one finger gait, it needs to be extended to a sequence of finger gaits that first achieves a grasp, whether precision or power, of the tool and then uses the tool to accomplish an intended task. This goal will require not only task planning at an even higher level to decompose an execution into finger gaits (and pivots) but also executions of more complex operations such as palm alignment and finger wrapping. More general gaits to include phalange under contact force modeling and control will present a bigger challenge. In the future, a library of executable gait sequences can be built for different hand tools with inspirations drawn from maneuvers by the human hand.

References

[1] J. Xu and Z. Li, "A kinematic model of finger gaits by multifingered hand as hybrid automation," in *IEEE Trans. Automat. Sci. Eng.*, vol. 5, no. 3, pp. 467–479, July 2018.

[2] Y. Fan, W. Gao, W. Chen, and M. Tomizuka. "Real-time finger gaits planning for dexterous manipulation," *IFAC-PapersOnLine*. vol. 50, pp. 12765–12772, 2017.

[3] J. Hong, G. Lafferriere, B. Mishra, and X. Tan, "Fine manipulation with multifinger hands," in *Proc. IEEE Int. Conf. Robot. Autom.*, 1990, pp. 1568–1573.

[4] L. Han and J. C. Trinkle, "Dexterous manipulation by rolling and finger gaiting," in *Proc. IEEE Int. Conf. Robot. Autom.*, 1998, pp. 730–735.

[5] S. LaValle and J. Kuffner, "Randomized kinodynamic planning," *Int. J. Robot. Res.*, 2012, vol. 20, no. 5, pp. 378–400.

[6] W. Bircher, A. Morgan, and A. Dollar. "Complex manipulation with a simple robotic hand through contact breaking and caging," *Science Robotics*. vol. 6, pp. eabd2666, 2021.

[7] R. Ma and A. Dollar. "An underactuated hand for efficient finger-gaiting-based dexterous manipulation," *Proc. IEEE Int. Conf. Robot. Biomim.*, 2014, pp. 2214–2219.

[8] A. Morgan, K. Hang, B. Wen, K. Berkris, and A. Dollar. "Complex In-Hand Manipulation via Compliance-Enabled Finger Gaiting and Multi-Modal Planning," *IEEE Robot. Autom. Lett.*, vol. 7, pp. 4821–4828, 2022.

[9] M. Huber and R. Grupen. "Robust finger gaits from closed-loop controllers," in *Proc. IEEE/RSJ Int. Conf. Intell. Robots and Syst.*, 2002, pp. 1578–1584.

[10] M. Pfanne, M. Chalon, F. Stulp, H. Ritter, and A. Albu-Schäffer. "Object-Level Impedance Control for Dexterous In-Hand Manipulation," *IEEE Robot. Autom. Lett.*, vol. 5, pp. 2987–2994, 2020.

[11] Y. Xue and Y.-B. Jia, "Gripping a cutting knife on the cutting board," *Proc. IEEE/RSJ Int. Conf. Intell. Robots and Syst.*, 2020, pp. 9226–9231.

[12] N. C. Dafle, A. Rodriguez, R. Paolini, B. Tang, S. S. Srinivasa, M. Erdmann, M. T. Mason, I. Lundberg, H. Staab, and T. Fuhlbrigge, "Extrinsic dexterity: In-hand manipulation with external forces," in *Proc. IEEE Int. Conf. Robot. Autom.*, 2014, pp. 1578–1585.

[13] D. L. Brock, "Enhancing the dexterity of a robot hand using controlled slip," in *Proc. IEEE Int. Conf. Robot. Autom.*, 1988, pp. 249–251.

[14] Y. Aiyama, M. Inaba, and H. Inoue, "Pivoting: A new method of graspless manipulation of object by robot fingers," in *Proc. IEEE/RSJ Int. Conf. Intell. Robots and Syst.*, 1993, pp. 136–141.

[15] A. Rao, D. J. Kriegman, and K. Y. Goldberg, "Complete algorithms for feeding polyhedral parts using pivot grasps," *IEEE Trans. Robot. Autom.*, vol. 12, no. 2, pp. 331–342, 1996.

[16] A. Holladay, R. Paolini, and M. T. Mason, "A general framework for open-loop pivoting," in *Proc. IEEE Int. Conf. Robot. Autom.*, 2015, pp. 3675–3681.

[17] Y. Hou, Z. Jia, A. M. Johnson, and M. T. Mason, "Robust plana dynamic pivoting by regulating inertial and grip forces," in *Algorithmic Foundations of Robotics XII*, 2020, pp 464–479, Springer, Cham..

[18] F. E. Vina, Y. Karayiannidis, C. Smith, and D. Kragic, "Adaptive control for pivoting with visual and tactile feedback," in *Proc. IEEE Int. Conf. Robot. Autom.*, 2016, pp. 399–406.

[19] Cruciani, S. & Smith, C., "In-hand manipulation using three-stages open loop pivoting," *IEEE/RSJ Int. Conf. Intell. Robot. Syst.*, 2017, pp. 1244-1251

[20] M. Raibert and J. Craig. "Hybrid position/force control of manipulators," *ASME J. Dyn. Syst. Meas. Control*, 1981, vol. 103, pp. 126–133.

[21] N. Hogan, "Impedance control: An approach to manipulation: Part I - Theory," 1985.

[22] N. Hogan, "Stable execution of contact tasks using impedance control," *Proc. IEEE Int. Conf. Robot. Autom.*, 1987, 4, pp. 1047-1054.

[23] T. Wimboeck, C. Ott and G. Hirzinger, "Passivity-based object-level impedance control for a multifingered hand," *Proc. IEEE/RSJ Int. Conf. Intell. Robots and Syst.*, 2006, pp. 4621-4627.

[24] K. Mirza and D. E. Orin, "General formulation for force distribution in power grasp," in *Proc. IEEE Int. Conf. Robot. Autom.*, 1994, pp. 880–887.

[25] Y. Yu, K. Takeuchi, and T. Yoshikawa, "Optimization of robot hand power grasps," in *Proc. IEEE Int. Conf. Robot. Autom.*, 1998, pp. 3341–3347.

[26] O. M. Ismaeil and R. E. Ellis, "Grasping using the whole finger," in *Proc. IEEE Int. Conf. Robot. Autom.*, 1994, pp. 3111–3116.

[27] Khatib, O. "A unified approach for motion and force control of robot manipulators: The operational space formulation," *J. Robot. Autom.*, 1987, vol. 3, pp. 43–53.

[28] M. Huber and R. A. Grupen, "Robust finger gaits from closed-loop controllers," in *Proc. IEEE/RSJ Int. Conf. Intell. Robots and Syst.*, 2002, pp. 1578–1584.

[29] M. Pfanne, M. Chalon, F. Stulp, H. Ritter, and A. Albu-Schäffer, "Object-level impedance control for dexterous in-hand manipulation," *IEEE Robot. Automat. Lett.*, 2020, vol. 5, no. 2, pp. 2987–2994.

[30] L. Biagiotti, H. Liu, G. Hirzinger & C. Melchiorri, "Cartesian impedance control for dexterous manipulation," *Proc. IEEE/RSJ Int. Conf. Intell. Robots and Syst.*, 2003, pp. 3270-3275.

[31] R. Anderson, and M. Spong, "Hybrid impedance control of robotic manipulators," *IEEE J. Robot. Autom.*, 1988, 4, 549-556.

[32] S. Jung, T. Hsia, and R. Bonitz, "Force tracking impedance control of robot manipulators under unknown environment," *IEEE Trans. Control Syst. Tech.*, 2004, 12, 474-483.

[33] E. Todorov, T. Erez, and Y. Tassa, "Mujoco: A physics engine for model-based control," *IEEE/RSJ Int. Conf. Intell. Robot. Syst.*, 2012, pp. 5026-5033.

[34] A. Wächter, and L. Biegler, "On the implementation of an interior-point filter line-search algorithm for large-scale nonlinear programming," *Mathematical Programming*, 2006, 106, 25-57.

[35] Shoemake, K., "Animating rotation with quaternion curves," *Proceedings Of The 12th Annual Conference On Computer Graphics And Interactive Techniques*. pp. 245-254.